Generation of Magnetic Field by Combined Action of Turbulence and Shear

T. A. Yousef,[1] T. Heinemann,[1] A. A. Schekochihin,[2] N. Kleeorin,[3]
I. Rogachevskii,[3] A. B. Iskakov,[4,2,5] S. C. Cowley,[4,2] and J. C. McWilliams[6]

[1]*DAMTP, University of Cambridge, Cambridge CB3 0WA, United Kingdom*
[2]*Plasma Physics Group, Blackett Laboratory, Imperial College, London SW7 2AZ, United Kingdom*
[3]*Department of Mechanical Engineering, The Ben-Gurion University of the Negev, P. O. Box 653, Beer-Sheva 84105, Israel*
[4]*Department of Physics and Astronomy, UCLA, Los Angeles, California 90095-1547, USA*
[5]*Wolfgang Pauli Institute, Universität Wien—UZA 4, Nordbergstraße 15, A 1090 Wien, Austria*
[6]*Department of Atmospheric Sciences, UCLA, Los Angeles, California 90095-1565, USA*

(Dated: October 17, 2007)

The possibility of a mean-field dynamo in nonhelical turbulence with superimposed linear shear is studied numerically in elongated shearing boxes. Exponential growth of magnetic field at scales much larger than the outer scale of the turbulence is found. The charateristic scale of the field is $l_{\overline{B}} \propto S^{-1/2}$ and growth rate is $\gamma \propto S$, where S is the shearing rate. This newly discovered form of large-scale dynamo action may have an extremely broad range of applications to astrophysical systems with spatially coherent mean flows.

PACS numbers: 47.65.Md, 47.27.W-, 95.30.Qd, 98.62.En

Introduction. Understanding the origin of cosmic magnetism is one of the fundamental theoretical challenges in astrophysics. The turbulent motions of the plasmas that make up most astrophysical objects are believed to be responsible for the generation of the magnetic field. In particular, a generic property of the turbulence of conducting fluid is to exponentially amplify magnetic fluctuations at the turbulence scales or smaller via the fluctuation dynamo effect [1, 2, 3, 4]. A distinct problem is to explain the observed presence in most astrophysical bodies of magnetic fields spatially coherent at scales larger than the outer scale of the turbulence (mean fields). Nonhelical homogeneous isotropic turbulence on its own cannot give rise to a mean field. What are then the large-scale properties that must be present in a turbulent system for such a field to be generated? Mean-field dynamo theories [5] have identified a number of amplification mechanisms. We know, e.g., that nonzero net helicity (often combined with rotation in real systems) is sufficient to produce mean fields, but is it necessary?

Perhaps the simplest and most common large-scale feature is mean shear. This arises in systems as varied as, e.g., stellar interiors [6], accretion disks [7], galaxies (in particular, irregular ones [8]), and liquid-metal laboratory dynamos [9], all of which host both large-scale (mean) and small-scale (fluctuating) magnetic fields. A number of theoretical arguments have proposed that a mere combination of turbulence and shear could give rise to a mean-field dynamo: e.g., the shear-current effect [10] and the stochastic α effect [11] (see also [12]). The shear-current-effect calculation in particular, where the τ-approximation closure was used, has provoked a debate because its results seemed to contradict the rigorous mean field theory based on the second-order correlation approximation (SOCA), which ruled out the shear dynamo [13, 14]. However, the SOCA is only strictly valid in the limit either of low hydrodynamic and magnetic Reynolds numbers, $\mathrm{Re}, \mathrm{Rm} \ll 1$, or short velocity correlation times [13]. In real turbulent systems, neither of these assumptions is satisfied, and the hope that some of the results qualitatively carry over has had to be backed up by numerical evidence [15] and by intuitive physical pictures of how the field is amplified [16]. The negative SOCA result for the shear dynamo is a quantitative one: the sign of a certain coefficient in the mean electromotive force turns out to be unfavorable. There is no reason why this should still be true outside the parameter regimes in which SOCA is valid. In the absence of a mechanistic model of the shear dynamo or of a physical argument for its impossibility or of a rigorous method for proceeding analytically, a numerical test appears to be called for. In this Letter, we report a series of numerical experiments in which the combination of imposed linear velocity shear and forced small-scale turbulence does give rise to a growing large-scale magnetic field.

Numerical Set Up. We consider the equations of incompressible magnetohydrodynamics (MHD) with a background linear shear flow $\mathbf{U} = Sx\hat{\mathbf{y}}$ and a white-noise nonhelical random homogeneous isotropic body force $\mathbf{f}$:

$$\frac{d\mathbf{u}}{dt} = -u_x S\hat{\mathbf{y}} - \frac{\nabla p}{\rho} + \frac{\mathbf{B}\cdot\nabla\mathbf{B}}{4\pi\rho} + \nu\nabla^2\mathbf{u} + \mathbf{f}, \quad (1)$$

$$\frac{d\mathbf{B}}{dt} = B_x S\hat{\mathbf{y}} + \mathbf{B}\cdot\nabla\mathbf{u} + \eta\nabla^2\mathbf{B}, \quad (2)$$

where $\mathbf{u}$ and $\mathbf{B}$ are the velocity and magnetic fields, $d/dt = \partial_t + Sx\partial_y + \mathbf{u}\cdot\nabla$, the density $\rho = 1$, and the pressure p is determined by the incompressibility condition $\nabla\cdot\mathbf{u} = 0$. These equations are solved with shear-periodic boundary conditions by a Lagrangian spectral method [17]. When the imposed shear S is weak compared to the turnover rate of the turbulent motions, the

TABLE I: Index of runs

S	L_z	Resolution	$u_{\rm rms}$	γ	$l_{\overline{B}}$	$\overline{B}_y/\overline{B}_x$ [a]
2	8	$32^2\times 256$	0.88	0.0161	3.7	6.54
2	16	$32^2\times 512$	1.06	0.021	3.8	6.49
1	8	$32^2\times 256$	0.70	0.0027	4.6	6.41
1	16	$32^2\times 512$	1.21	0.0124	5.4	6.50
1	32	$32^2\times 1024$	1.01	0.0092	5.2	6.43
1	64	$32^2\times 2048$	1.06	0.0093	5.1	6.38
0.5	16	$32^2\times 512$	0.74	0.0040	6.8	6.34
0.5	32	$32^2\times 1024$	1.11	0.0052	7.0	6.21
0.25	32	$32^2\times 1024$	0.95	0.00184	9.9	6.15
0.25	64	$32^2\times 2048$	0.77	0.0023	10.6	6.12
0.25	128	$32^2\times 4096$	0.76	0.0027	10.9	6.10
0.125	64	$32^2\times 2048$	0.66	0.00107	13.5	6.13

[a] Here we give the time average of $\left[\int dz\overline{B}_y^2(z)/\int dz\overline{B}_x^2(z)\right]^{1/2}$.

growth of the mean (large-scale) field can only be detected if the size of the computational domain is much larger than the turbulence scale l_0. In general, this, together with the necessity to run the simulations for very long times, requires unaffordable amounts of computing power. We circumvent this problem by using computaional boxes with large aspect ratios, $L_x\times L_y\times L_z$, where $L_z\gg L_x=L_y$. The units of length and time are fixed by setting $L_x=L_y=1$ and the mean forcing power $\epsilon=\langle\mathbf{u}\cdot\mathbf{f}\rangle=1$ (this can be controlled because the forcing is white-noise). The forcing scale is $l_0=1/3$, i.e., the energy is injected in the wave-number shell $k_0/2\pi=3$. The resulting root-mean-square velocity field is $u_{\rm rms}\equiv\langle u^2\rangle^{1/2}\sim 1$, so the typical turnover rate of the turbulent motions is $u_{\rm rms}/l_0\sim 3$. We study five values of the shear $S=2,1,1/2,1/4,1/8<u_{\rm rms}/l_0$. The viscosity and magnetic diffusivity are $\nu=\eta=10^{-2}$, so $\mathrm{Rm}=\mathrm{Re}\equiv u_{\rm rms}/k_0\nu\sim 5$. The resolution requirements are consequently not large: it suffices to have 32×32 collocation points in the (x,y) plane. In the z direction, we use resolutions between 256 and 4096 collocation points for $L_z=8,\dots,128$, depending on S (Tab. I).

Strictly speaking, we cannot speak about turbulence with such low Re. However, a developed inertial range is not important for mean field dynamos: it is sufficient that a stochastic velocity field with $\mathrm{Re}\gtrsim 1$ is present.[22] In our simulations, Rm is subcritical with respect to the fluctuation dynamo [2, 3, 4], so any field growth we detect is due purely to a mean-field dynamo. Note, however, that since $\mathrm{Rm}>1$, turbulent tangling of the mean field generates small-scale magnetic fluctuations whose energy is in general larger than that of the mean field [4].

Results. We find that magnetic field grows exponentially with time at all values of S studied, provided the computational box is sufficiently long. For each value of S, we consider the growth rate γ of $B_{\rm rms}\equiv\langle B^2\rangle^{1/2}$

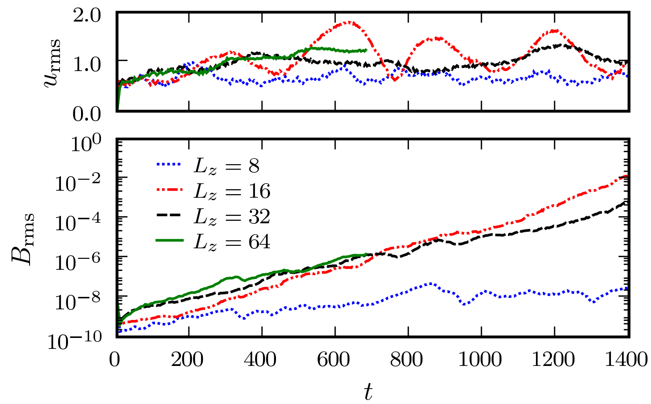

FIG. 1: Evolution of $u_{\rm rms}$ (upper panel) and $B_{\rm rms}$ (lower panel) for $S=1$ and four values $L_z=8,16,32,64$.

converged if it stays approximately the same when L_z is doubled (Fig. 1). That we are able to find such values means that the growth of the field is asymptotically independent of L_z (the dependence on L_x and L_y should also be studied but that is currently too expensive computationally). The exponential growth of the magnetic field eventually brings it to dynamically strong saturated levels. In this paper, we will concentrate on the kinematic (weak-field) regime and leave the properties of the saturated state to a future study.

Fig. 2 shows that, in the range of shears studied, the growth rate of $B_{\rm rms}$ increases linearly with S, $\gamma\propto S$. From the theoretical point of view, this is a somewhat unexpected result because the shear-current effect [10], as well as most other mean-field theories quoted above predict $\gamma\propto S^2$ for the fastest-growing mode.

That the growing field is large-scale is obvious already from the visualization of the field: the large-scale z-dependent modulation is evident against the turbulence-scale structure (Fig. 3). We isolate this large-scale dependence on z by low-pass filtering in Fourier space:

$$\overline{\mathbf{B}}(z)=\sum_{|k_z|<1}\mathbf{B}(k_x=0,k_y=0,k_z)\,e^{ik_zz}. \qquad (3)$$

Note that since $\nabla\cdot\mathbf{B}=0$, $\overline{B}_z=0$. This procedure averages out the small-scale structure and brings out the growing large-scale field in a clear way (Fig. 3). We note that in all cases, the root-mean-square values of $\overline{B}_x$ and $\overline{B}_y$ grow exponentially with the same rate γ as $B_{\rm rms}$. We also have $\overline{B}_y>\overline{B}_x$, which is expected because the shear systematically converts B_x into B_y [Eq. (2)]. The ratio $\overline{B}_y/\overline{B}_x\sim S/\gamma$ is approximately constant in time and its average is independent of S (Tab. I), which is consistent with $\gamma\propto S$ established above.

Examining Fig. 3, we see that the magnetic field grows in large random patches along the box. In time, these patches move around and change shape. Thus, it is not a "mode" with spatial profile constant in time, so the spatial structure of the large-scale field can only be described systematically in a statistical way. We define the

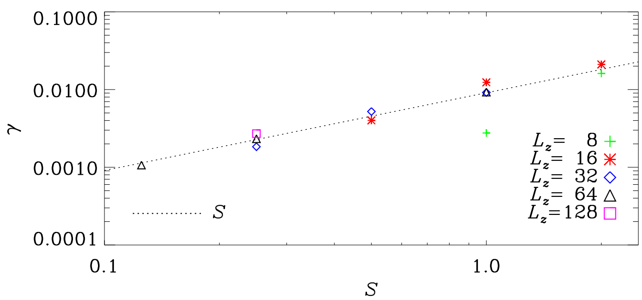

FIG. 2: Growth rates γ of $B_{\rm rms}$ for all runs (Tab. I). The dotted line shows the slope corresponding to $\gamma \propto S$.

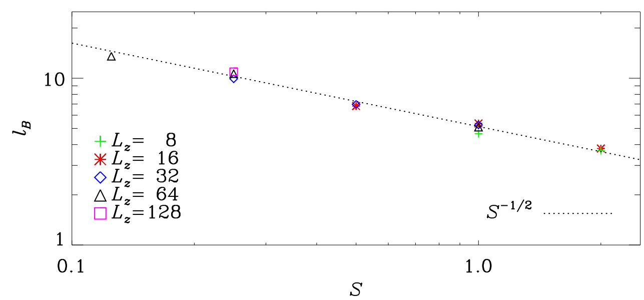

FIG. 4: The characteristic scale of the magnetic field [Eq. (4)] for all runs. The dotted line showes the slope $S^{-1/2}$.

time-averaged characteristic scale $l_{\overline{B}}$:

$$\frac{1}{l_{\overline{B}}} = \frac{1}{T}\int dt \left[\frac{\int dz\,(\partial \overline{B}_y/\partial z)^2}{\int dz \overline{B}_y^2}\right]^{1/2}. \quad (4)$$

Here and in all other cases, the time average is taken over the exponential-growth (kinematic) period of the field evolution. The derivatives are calculated in Fourier space. The values of $l_{\overline{B}}$ are given in Tab. I and plotted vs. S in Fig. 4. As the shear is decreased, $l_{\overline{B}}$ increases and is matched rather well by the scaling $l_{\overline{B}} \propto S^{-1/2}$.

This scaling again is at odds with the mean-field-theory prediction $l_{\overline{B}} \propto S^{-1}$ [10]. There is, however, a simple argument that shows that it is consistent with $\gamma \propto S$. Let us write the mean-field equations in the standard model form that is usually sought by analytical theories:

$$\partial_t \overline{B}_x = -\eta_T k_z^2 \overline{B}_x + A\overline{B}_y, \quad (5)$$
$$\partial_t \overline{B}_y = -\eta_T k_z^2 \overline{B}_y + S\overline{B}_x, \quad (6)$$

where $\eta_T \sim u_{\rm rms} l_0$ is the turbulent diffusivity and A is some operator that closes the dynamo loop (the main challenge of mean-feld theories is to find A). The growth rate is $\gamma = \sqrt{SA} - \eta_T k_z^2$. The wave number of the fastest-growing mode can be estimated by setting the two terms in this expression to be comparable, so, if $k_z \sim l_{\overline{B}}^{-1} \sim l_0^{-1}(Sl_0/u_{\rm rms})^{1/2}$, we have $A \sim S$ and $\gamma \sim S$. This argument suggests the possible form that a mean-field theory of the dynamo reported here may take.

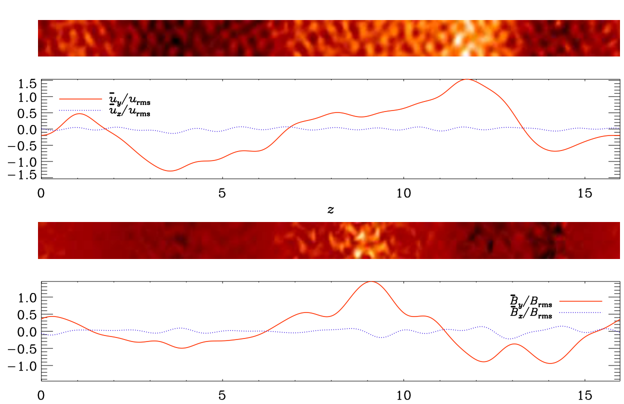

FIG. 3: Snapshots of u_y (upper panel) and B_y (lower panel) taken in an (y, z) cross-section of the $L_z = 16$ run for $S = 1$. Underneath the snapshots are plots of $\overline{u}_y(z)$, $\overline{u}_x(z)$ (upper panel) and $\overline{B}_y(z)$, $\overline{B}_x(z)$ (lower panel). Here $\overline{\mathbf{u}}(z)$ is defined similarly to $\overline{\mathbf{B}}(z)$ [Eq. (3)].

Finally, in Fig. 5, we show the one-dimensional spectrum of magnetic energy during the growth stage. It is strongly peaked at large scales ($k_z l_0 \ll 1$), but also shows that the mean field is tangled by the turbulence to produce a significant amount of magnetic energy at the turbulence scales.

Effect of Shear on the Velocity Field. If shear combined with turbulence can give rise to large-scale magnetic fields, a similar mechanism may also lead to growing large-scale velocity structures (a "vorticity dynamo" [18]). This does, indeed, seem to occur: the velocity field develops large fluctuations that are energetically comparable to the small-scale turbulence, last for long times (Fig. 1) and are spatially coherent on scales similar to those of the magnetic field (Fig. 3). The large-scale structure forms mainly in the u_y component (corresponding to large-scale vorticity, $\overline{\omega}_x = -\partial\overline{u}_y/\partial z$). This process is nonlinear at all times (there is no "kinematic" stage

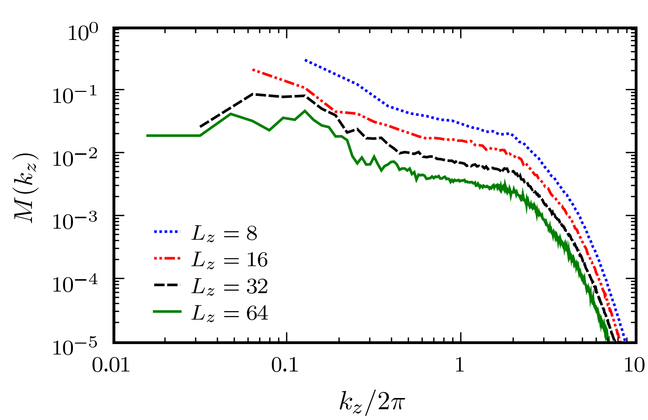

FIG. 5: Normalized one-dimensional spectra of the magnetic energy, $M(k_z) = \sum_{k_x,k_y} |\mathbf{B}(k_x,k_y,k_z)|^2/\langle B^2\rangle$ (time averaged over the growth stage) for $S = 1$ and $L_z = 8, 16, 32, 64$. The four graphs demonstrate that, as L_z is increased, a large-scale spatial structure independent of the box length emerges.

when the vorticity is dynamically insignificant). Its detailed study is outside the scope of this Letter.

Although it is not clear whether the shear-generated large-scale velocity structures play a role in the magnetic-field amplification, the growth of the field does not seem to be strongly correlated with their presence (compare, e.g., the time evolution of $u_{\rm rms}$ and $B_{\rm rms}$ in Fig. 1).

Finally, we note that the presence of shear can lead to nonlinear destabilization of finite perturbations of the velocity field and formation of shear-driven turbulence whose outer scale is the scale of the shear (in simulations with a linear shear, the box scale). This does indeed happen in our simulations when S is too strong or the box is too long. The quantitative signature of this regime is that the power input from the shear in Eq. (1), $-\langle u_x u_y\rangle S$, exceeds the forcing power $\epsilon = \langle \mathbf{u}\cdot\mathbf{f}\rangle$. We avoid this regime to isolate the mean-field generation effect, which requires a scale separation between the turbulence and the mean field. In all runs reported here, $|\langle u_x u_y\rangle S| \ll \epsilon$. We note that the large upward fluctuations of $u_{\rm rms}$ [Fig. 1] are not accompanied by a significant change in $\langle u_x u_y\rangle S$, so the large-scale velocity structures appear to feed on the forcing power, not on the power extracted from the shear.

Discussion. We have found that a large-scale magnetic field grows exponentially in long sheared boxes with forced small-scale nonhelical turbulence. In the parameter range we have studied, the growth rate is $\gamma \propto S$, the spatial scale of the field $l_{\overline{B}} \propto S^{-1/2}$ and $\overline{B}_y/\overline{B}_x \simeq \text{const} > 1$ (independent of S). These properties do not seem to fit any of the existing theoretical predictions. Our results do, however, lend credence to the concept of a shear-driven dynamo and thus should provide motivation for further theoretical effort.

To our knowledge, this is the first demonstration of the shear dynamo effect in a dedicated numerical experiment. In an earlier unpublished study we obtained similar results using PENCIL code (a compressible finite-difference code in contrast to the spectral one used above), so the amplification effect appears to be numerically robust. We note that there have been earlier indications of nonhelical turbulence amplifying large-scale magnetic field in the presence of a large-scale shear associated with mean flows in numerical experiments that used constant-in-time sinusoidal forcing functions [19, 20]. Another example of large-scale magnetic fields generated by a combination of nonhelical turbulence and a mean flow is the numerical experiments with Taylor-Green forcing [21]. One might speculate that the shear provided by the mean flow in such systems could act in a way qualitatively similar to a linear shear and give rise to mean-field amplification.

As the combination of a mean flow and turbulence is a very common situation in natural systems, the shear dynamo potentially represents a very generic mechanism for making large-scale fields. While much needs to be understood about its properties before applications to real astrophysical systems can be anything more than an appealing speculation, the simplicity of the idea of shear dynamo certainly makes it a worthwhile object of study.

We thank A. Brandenburg, L. Kitchatinov, G. Ogilvie, J. Papaloizou, F. Rincon, D. Shapovalov and D. Sokoloff for valuable discussions. Simulations were done on UKAFF (Leicester), NCSA (Illinois) and Cambridge HPCF. This work was supported by STFC (T.H., A.A.S), UKAFF (T.A.Y.), Newton Trust (T.A.Y, T.H.), US DOE Center for Multiscale Plasma Dynamics (A.B.I., S.C.C.), the Royal Society (I.R., A.B.I.) and the Leverhulme Trust International Network for Magnetized Plasma Turbulence.

[1] G. K. Batchelor, Proc. R. Soc. London A **201**, 405 (1950); A. P. Kazantsev, Sov. Phys.–JETP **26**, 1031 (1968); Ya. B. Zeldovich, A. A. Ruzmaikin, and D. D. Sokoloff, *The Almighty Chance* (World Scientific, Singapore, 1990); M. Meneguzzi, U. Frisch, and A. Pouquet, Phys. Rev. Lett. **47**, 1060 (1981).
[2] A. A. Schekochihin et al., Astrophys. J. **612**, 276 (2004).
[3] A. B. Iskakov et al., Phys. Rev. Lett. **98**, 208510 (2007).
[4] A. A. Schekochihin et al., New J. Phys. **9**, 300 (2007).
[5] F. Krause and K.-H. Rädler, *Mean-Field Magnetohydrodynamics and Dynamo Theory* (Pergamon Press, New York, 1980); H. K. Moffatt, *Magnetic Field Generation in Electrically Conducting Fluids* (Cambridge University Press, Cambridge, 1978); A. Brandenburg and K. Subramanian, Phys. Rep. **417**, 1 (2005).
[6] M. Ossendrijver, Astron. Astrophys. Rev. **11**, 287 (2003).
[7] J.-F. Donati et al., Nature **438**, 466 (2005).
[8] K. T. Chyzy et al., Astron. Astrophys. **355**, 128 (2000); B. M. Gaensler et al., Science **307**, 1610 (2005).
[9] R. Monchaux et al., Phys. Rev. Lett. **98**, 044502 (2007).
[10] I. Rogachevskii and N. Kleeorin, Phys. Rev. E **68**, 036301 (2003); Phys. Rev. E **70**, 046310 (2004).
[11] M. R. E. Proctor, e-print arXiv:0708.3201.
[12] V. Urpin, Mon. Not. R. Astron. Soc. **308**, 741 (1999); Phys. Rev. E **65**, 026301 (2002); G. Rüdiger and V. Urpin, Astron. Astrophys. **369**, 323 (2001).
[13] K.-H. Rädler and M. Rheinhardt, Geophys. Astrophys. Fluid Dyn. **101**, 117 (2007).
[14] K.-H. Rädler and R. Stepanov, Phys. Rev. E **73**, 056311 (2006); G. Rüdiger and L. L. Kitchatinov, Astron. Nachr. **327**, 298 (2006).
[15] A. Brandenburg, Astrophys. J. **550**, 824 (2001).
[16] E. N. Parker, Astrophys. J. **122**, 293 (1955).
[17] G. I. Ogilvie, unpublished (1998); Y. Lithwick, e-print astro-ph/0702046.
[18] T. Elperin, N. Kleeorin, and I. Rogachevskii, Phys. Rev. E **68**, 016311 (2003).
[19] A. Brandenburg, Astrophys. J. **625**, 539 (2005).
[20] D. Shapovalov, private communication (2006).
[21] Y. Ponty et al., Phys. Rev. Lett. **94**, 164502 (2005); P. D. Mininni et al., Astrophys. J. **626**, 853 (2005).
[22] It is also important that Re and Rm are not too small. We found that the shear dynamo effect disappears at low Re and Rm, as predicted by SOCA [14].